24th COBEM - 2017

24th ABCM International Congress of Mechanical Engineering
December 3-8, 2017, Curitiba, PR, Brazil

COBEM-2017-2657
SIMULATION OF CASTING PROCESS OF MARINE PROPELLERS

Helder Monteiro Santana
Erb Ferreira Lins
Federal University of Pará, Faculty of Mechanical Engineering, St. Augusto Corrêa, 01 - Guamá, CEP 66075-110, Belém, Pará, Brazil.
heldersantana10@hotmail.com, erb@ufpa.br

Abstract. *Producing marine propellers are very important to the Amazon, mainly because it is the largest navigable river of the world. The most common problems found in boats of the region are the lack of technical procedures for the propellers' design. During the casting process, it is very common to observe micro-structural defects. In this paper, a numerical approach is applied to the study of solidification of metallic alloys during the casting process of marine propellers. The aiming is an evaluation of a liquid-solid interface that advances in heat extraction direction, in order to improve this process. A small marine propeller with 0.26 m diameter was computationally built. An optimized procedure was used to get the blade hydrodynamic shape. Simulations using the finite volume method were performed with ANSYS FLUENT. The solidification of fluid phase and heat transfer within the metal-cast was analyzed taking into account a computational sand mold. As a result, the temperature gradient in the three-dimensional space and cooling curves at any point of the propeller was obtained. The solidification is faster at the blade tip than close to the shaft. The proposed modeling shows physical consistency, demonstrating that it may be used in the microstructural characterization of solidified metal.*

Keywords: *Solidification, Heat Transfer, Finite Volume Method.*

1. INTRODUCTION

The Amazon region is well-known due to its variety of rivers, minerals and vast biodiversity. According to Favacho (2014), the Amazon is the largest navigable river of the world, as well as the longest in length and largest in water flow, in which the navigation is the main means of transportation. Also, it is characterized by the presence of several towns and riverside communities (Lopes, 2003; Loureiro *et al.*, 2000).

Most boats use propeller-type propulsion system, in which a circular-shaped element rotates around shaft, causing the blades to produce a displacement of the body of water, and then the movement of the boat. These propellers are usually manufactured through casting process because of their versatility and low production cost. However, this process is carried out with heavily empiricism, generating unsatisfactory mechanical behavior due to the presence of microstructural defects such as cracks, porosity, voids, etc. generally formed during the solidification of the material (Loureiro *et al.*, 2000).

Therefore, this work presents a numerical analysis of the solidification process of marine propellers, using the finite volume method through the software ANSYS FLUENT. The approach allows to evaluate the heat transfer in the liquid-solid transition, as well as the phase changing in the metal alloy. The heat in the metal-mold interface and the transfer of heat out of the mold are also determined. The results show the temperature variation in the transient regime at any point in the propeller-mold, permitting to estimate microstructures after solidification of the molten material.

2. NUMERICAL METHODOLOGY

2.1 Geometry of the propeller and sand mold

In the casting process of marine propellers, a typical sand mold is built from a propeller model under desired dimensions. The mold (under $300K$) is placed on a solid surface, so that through a channel, it receives liquid metal. Then the Al-3wt.%Si metal alloy is casted at $919.15K$ in the mold. At this time, the solidification process begins due to the cooling generated by the heat extraction from the mold (Fig. 1). The lateral and upper walls in contact with the free air at $300K$ undergo the natural convection phenomenon, whose convection coefficient is of $11.45W/m^2.K$. After a certain period of time, the metal alloy solubilizes and the mold is withdrawn, thereby obtaining the propeller.

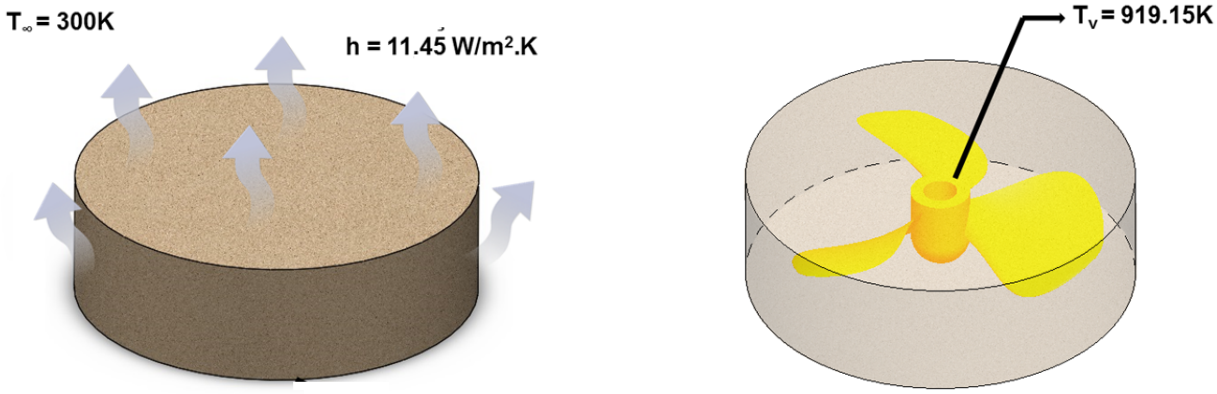

(a) (b)

Figure 1. (a) Extraction of heat from sand mold; (b) Translucent vision of the sand mold.

The propeller geometry was designed based on the optimized propeller model made by Favacho (2014), which is similar to the propellers used by small boats of the Amazon region. From chord and twist angle values corresponding to the radial distance of 10 equally spaced cross sections, a computational algorithm executed in MATLAB software transformed these data into 1000 sublevels, which describe the hydrofoil of each blade section. So, the data were imported to the software SOLIDWORKS, where the propeller was constructed (Fig. 2(a)). Only one third of the geometry was generated, in order to consider its symmetry, reducing the computational time-consume. In the ANSYS softwere, the mold was built next to the propeller with a mesh of $4,168,942$ elements and $782,649$ nodes (Fig. 2(b)).

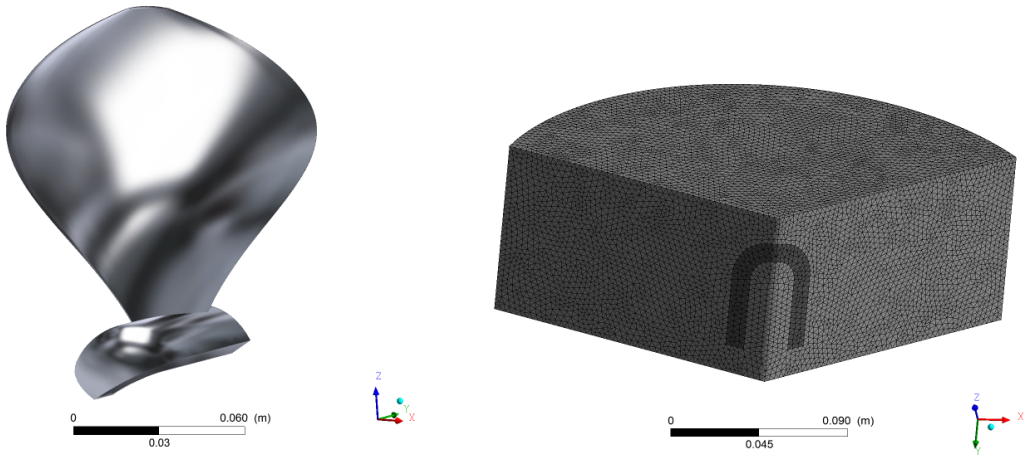

(a) (b)

Figure 2. (a) One third of the propeller geometry; (b) Computational mesh of the propeller-mold system.

Table 1 presents the main dimensions of the propeller geometry obtained in the SOLIDWORKS software.

Table 1. Dimensions and characteristics of the naval propeller

Propeller diameter	0.264 m
Boss inner diameter	0.026 m
Boss outer diameter	0.046 m
Number of blades	3
Airfoil profile	NACA 16006

2.2 Materials, computational modeling and boundary conditions

Table 2 presents the main thermophysical properties of pure aluminum, silicon and AI 50/60 AFS industrial sand involved in the solidification process. The experimental data of pure aluminum obtained in the work of Gandin (2000) show that the density, specific heat and thermal conductivity properties vary with temperature, as these values were

interpolated and transformed into the MATLAB software in polynomial functions. The same procedure was done for the specific heat and thermal conductivity data of the silicon purchased in Ioffe. AI 50/60 AFS industrial sand has thermophysical properties similar to green sand. In addition, there is little variation of these properties when submitted to different temperatures, which were obtained in the work of Pariona and Mossi (2005).

Table 2. Thermo-physical properties of materials

Pure Aluminum	
Density (Kg/m^3)	$2,535,\ if\ 300K \leq T \leq 933.35K$
	$2,370,\ if\ 933.35K < T \leq 1500.15K$
Specific Heat $(J/Kg.K)$	$852.14945 + 0.378651T, if\ 300K \leq T \leq 933.35K$
	$1,205.857 - 0.128428T,\ if\ 933.35K < T \leq 1,500K$
Thermal Conductivity $(W/m.K)$	$232.1236 + 0.04336897T - 7.179566 \times 10^{-5}T^2,\ if\ 300K \leq T \leq 933.35K$
	$46.45382 + 0.05889061T - 1.231604 \times 10^{-5}T^2,\ if\ 933.35K < T \leq 1,500K$
Dynamic Viscosity $(Kg/m.s)$	1.72×10^{-5}
Latent heat (J/kg)	$385,000$
Melting temperature (K)	933.35
Silicon	
Density (Kg/m^3)	$2,330$
Specific Heat $(J/Kg.K)$	$921.6984 - 0.6900467T + 0.001042T^2 - 7.156777 \times 10^{-7}T^3 + 1.8922 \times 10^{-10}T^4,\ if\ 300K \leq T \leq 1,000K$
	$821.7375 - 0.183932T + 0.000143T^2 - 3.776221 \times 10^{-8}T^3 + 3.3584 \times 10^{-12}T^4,\ if\ 1,000K < T \leq 4,000K$
Thermal Conductivity $(W/m.K)$	$707.9228 - 2.994143T + 0.0049859T^2 - 2.969095 \times 10^{-6}T^3,\ if\ 219.1595K \leq T \leq 625.39K$
	$-70.9706 + 0.78127T - 0.00147T^2 + 1.051 \times 10^{-6}T^3 - 2.607 \times 10^{-10}T^4,\ if\ 625.39K < T \leq 1,503.24K$
Industrial Sand AI 50/60 AFS	
Density (Kg/m^3)	$1,494.71$
Specific Heat $(J/Kg.K)$	$1,172.3$
Thermal Conductivity $(W/m.K)$	0.52

When the Al-3wt.%Si alloy is formed, the thermophysical properties of the pure aluminum and silicon are mixed and new ones are obtained, which can be calculated from the Al-Si diagram shown in Fig. 3.

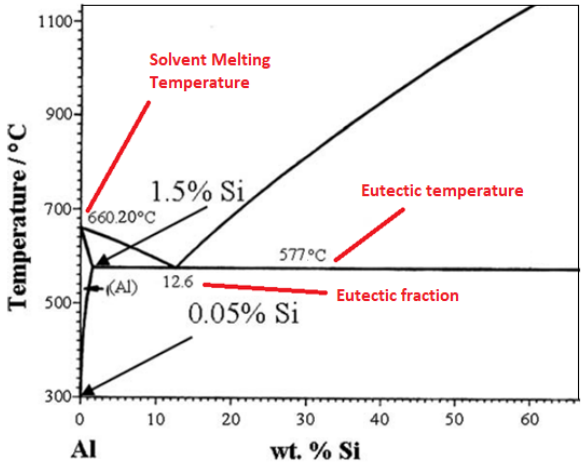

Figure 3. Phase diagram of Al-Si alloy.

Observing the diagram above, it is possible to infer the values of the eutectic temperature and the eutectic fraction. The slope of the liquidus line is calculated according to Eq. 1.

$$m = \frac{T_{Eut} - T_{melt}}{y} \tag{1}$$

where T_{Eut} is the eutectic temperature, T_{melt} is the melting temperature of the pure solvent and y is the eutectic fraction. Also the partition coefficient is obtained by

$$k = \frac{C_S}{C_L} \tag{2}$$

Then, C_S is the concentration of solute in the solid at the interface and C_L is the concentration of solute in the liquid at the interface. Thus, from the diagram of Fig. 3 and from Eq. 1 and 2 the values of Tab. 3 were obtained.

Table 3. Properties of alloy Al-3wt.%Si

Eutectic temperature	850.15K
Eutectic fraction	0.126
Slope of liquidus line	- 660.31746
Partition Coefficient	0.130723

In the process of solidification of metal alloys the formation of a region containing solid and liquid occurs. Regarding this pasty zone, FLUENT uses the formulation called enthalpy-porosity, in which it considers the conservation of energy through the enthalpy and the identification of the regions of liquid-solid transition through a pseudo porosity. The equations for the flow velocity of the liquid region are also considered. Thus, the solid-liquid pasty zone is treated as a porous zone with porosity equal to the liquid fraction and appropriate terms are added to the conservation equations of momentum, mass and energy to account for the formation of solid material. The pasty zone is a region in which the liquid fraction is between 0 and 1. As the material solidifies, that fraction tends to drop to 0 (ANSYS, 2013). FLUENT uses the Finite Volume Method, the most accurate numerical method for this type of problem.

The modeling presented in ANSYS (2013) shows that the enthalpy of the material is calculated as the sum of the sensible enthalpy, h, and the latent heat, $\triangle H$:

$$H = h + \triangle H \tag{3}$$

where

$$h = h_{ref} + \int_{T_{ref}}^{T} c_p dT \tag{4}$$

and h_{ref} is the reference enthalpy temperature, T_{ref} is the set point temperature and cp is the specific heat at constant pressure. The net fraction, β, is defined by

$$\begin{aligned} \beta &= 0 && if \quad T < T_{solidus} \\ \beta &= 1 && if \quad T > T_{liquidus} \\ \beta &= \frac{T - T_{solidus}}{T_{liquidus} - T_{solidus}} && if \quad T_{solidus} < T < T_{liquidus} \end{aligned} \tag{5}$$

The latent heat value ($\triangle H$) is written as a function of the latent heat of the material (L), according to Eq. 6.

$$\triangle H = \beta L \tag{6}$$

In solidification problems, the energy equation is written as

$$\frac{\partial}{\partial t}(\rho H) + \bigtriangledown \cdot (\rho \vec{v} H) = \bigtriangledown \cdot (k \bigtriangledown T) + S \tag{7}$$

where H is the enthalpy, ρ is the density, $\vec{v}$ is the fluid velocity and S is the source term.

The porosity, fortified by the enthalpy-porosity technique, is adjusted to the net fraction in each cell. Then the equation of the momentum is written:

$$S = \frac{(1-\beta)^2}{(\beta^3 + \varepsilon)} A_{mush} (\vec{v} - \vec{v}_p) \tag{8}$$

where β is the net fraction, ε is a constant (0.001), A_{mush} is the pasty zone constant, and V_p is the solid velocity due to the extraction of material solidified by the domain.

When mixing substances, the Species Equations model is used. In the metal alloy, as shown in the phase diagram of Fig.3, the solidus and liquidus temperatures determine the state of the material. These are calculated by:

$$T_{solidus} = T_{melt} + \sum_{solute} m_i Y_i / k_i \tag{9}$$

$$T_{liquidus} = T_{melt} + \sum_{solute} m_i Y_i \tag{10}$$

where k_i is the partition coefficient of solute i, Y_i is the mass fraction of solute i and m_i is the slope of the liquidus line of the respective Y_i.

In mixtures, the net fraction is calculated by

$$\beta^{n+1} = \beta^n - \lambda \frac{a_p (T - T^*) \triangle t}{\rho V L - a_p \triangle t L \frac{\partial T}{\partial \beta}}. \tag{11}$$

where n indicates the number of iterations, λ is the relaxation factor, a_p is the coefficient of the cell matrix, $\triangle t$ is the time-step, ρ is the density, V is the volume of the cell, T is the temperature of the cell, and T^* is the temperature at the interface.

The Scheil rule is used for species segregation at the micro scale. Thus the temperature at the interface is given by Eq.12.

$$T^* = T_{melt} + \sum_{i=0}^{N_s - 1} m_i Y_i \beta^{K_i - 1} \tag{12}$$

The FLUENT solidification model expresses the contact resistance of the region between the mold wall and the molten metal, using additional heat transfer resistance between the walls of the mold and cells with liquid fractions of less than 1 (Fig. 4). In this region, the heat flow becomes:

$$q = \frac{(T - T_w)}{(l/K + R_c(1 - \beta)} \tag{13}$$

In which T, T_w and l is defined in Fig. Ref fig6, K is the thermal conductivity of the fluid, β is the net fraction and R_c is the resistance of contact.

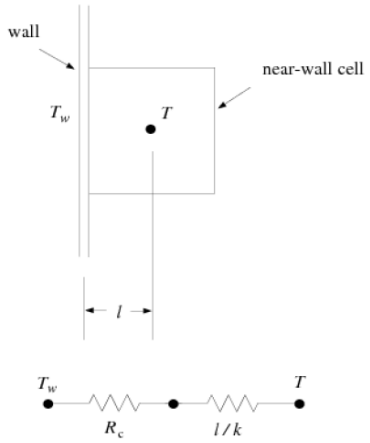

Figure 4. Circuit for contact resistance (ANSYS, 2013)

The simulated solidification regime was the transient, in which the acceleration of gravity adopted was of $9.81 m/s^2$. The initial temperature of the metal alloy was considered to be $919.15K$, while the mold was at a temperature of $300k$. In the upper and lateral wall of the mold was used the condition of convection contour, whose coefficient adopted is of $11.45 W/m^2.K$. For the surfaces that cut the propeller-mold system the condition of symmetry was used. Finally, the percentage of silica adopted was 3%.

3. RESULTS AND DISCUSSION

The numerical simulation of the solidification process was carried out in transient regime, providing results in different moments of cooling of the molten metal. Figure 3shows the three-dimensional temperature gradient for $100s$ of cooling. The trailing edge, leading edge and the propeller tip cool faster than the other parts (Fig. 5(a)), as the heat transfer is more pronounced due to the small thickness. The front surface of the cube occurs where there is a higher concentration of heat, because the contact region between the mold and the ground, in which natural convection does not act. The time result of $100s$ also shows the heating experienced by the mold (Fig. 5(b)). The sand around the propeller is heated around $660K$, while much of the mold is at $300K$. This occurrence is observed due to the low thermal conductivity of the material and the extraction generated by the natural convection in the walls of the mold.

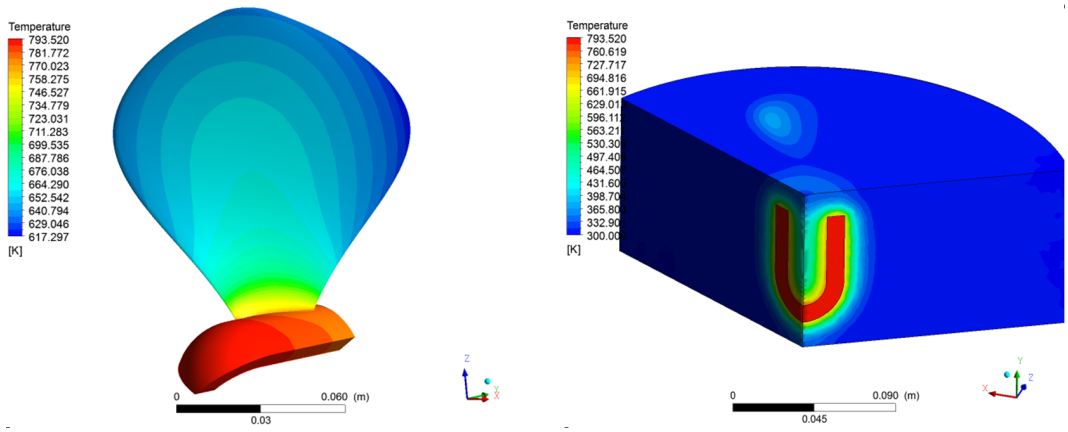

(a) (b)

Figure 5. Temperature gradient: (a) propeller of Al-3%Si after $100s$; (b) cast with fused propeller at instant $100s$.

The numerical values of liquid fraction and temperature in the cross-section of the propeller blade, at $10s$, $15s$ and 20, are shown in Fig. 6. In the first $10s$ the percentage of liquid at the ends of the blade section is zero, so in this region the material is in the solid phase. While in the center, the liquid fraction is around 12% (pasty). This pasty zone is still present because the temperature in this region is above eutectic temperature ($850.15K$). It is also important to note that the extraction of heat causes the fraction of liquid to cancel from the extremes to the center of the cross section, consequently, the material solidifies on that direction.

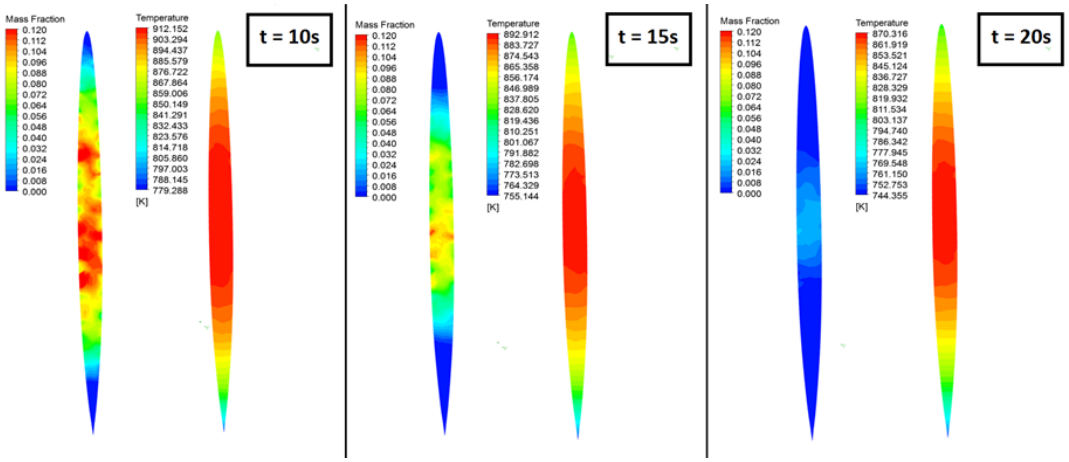

Figure 6. Liquid fraction and temperature of the propeller cross section at $10,\ 15$ and $20s$.

Figure 7(a) shows the temperature map of the radial section (Plane yz), where the temperature variation was measured at 3 points of the propeller and 4 points of the mold during the $300s$ of cooling. The results of this procedure are shown in the curves of Fig. 7(b). The propeller cooling and the heating and cooling of the sand mold are observed at such locations. At point 1, located at the tip of the blade, the temperature drop is more pronounced regarding the time dependence, while at points 2 and 3, positioned on the hub, cooling is slow. This is due to the higher speed of heat extraction. This event directly influences the size of the grain formed and, consequently, different crystalline microstructures will be formed in these regions.

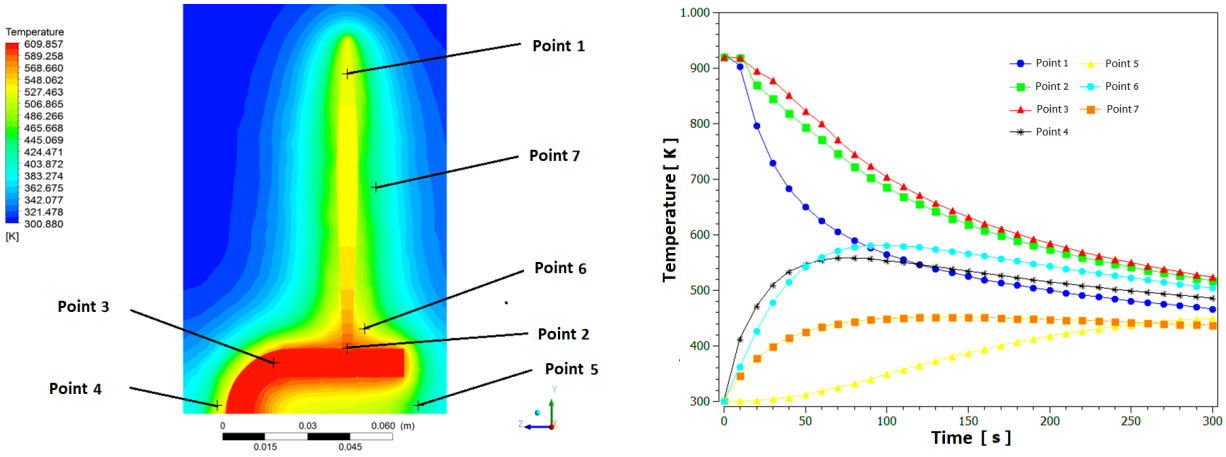

(a) (b)

Figure 7. (a) Temperature map of the longitudinal section of the propeller of Al-3wt.%Si after $300s$; (b) Curves of cooling/heating of the propeller-mold system.

As for the sand mold, it is possible to analyze that in the near points of the molten metal, the sand heating takes place until reaching a temperature plateau. From this moment, the mold begins to cool, since the heat diffuses slowly towards the walls, where natural convection occurs (Fig. 7(a)). Point 6, located near the root of the propeller, was the one that suffered the highest heating. Another point where the heating is large and fast is 4 because it is close to the contact surface between the mold and the soil where the heat transfer is slow. At points 5 and 7, the temperature rise slower due to the convection currents in the mold wall. It is noteworthy that there is no forced convection source acting on the propeller-mold system, so that the sand mold is the main temperature control mechanism, which influences the formation of the alloy microstructure.

4. CONCLUSION

In this work a computational methodology for the process of solidification of naval propellers was presented. The simulation showed the three-dimensional temperature distribution in transient regime, where the propeller cools primarily at the ends of the blade and the front face of the hub is the region with the highest heat concentration. It was also possible to evaluate the pasty zone of Al-3wt.% Si, where it was observed that the metal solidifies from the ends toward the center of the helix geometry, decreasing the percentage of liquid. This study was only feasible because of the enthalpy-porosity formulation employed by the software ANSYS FLUENT. In addition, the simulation generated cooling curves at some points of the propeller, which have different cooling rates and, consequently, different micro-structures must be formed in the solidified metal. In order to control the temperature, the properties of the mold should be considered, since the results showed that it is the main agent in the extraction of heat from the molten metal.

5. ACKNOWLEDGEMENTS

This work was supported by Federal University of Pará (UFPA).

6. REFERENCES

ANSYS, 2013. *ANSYS Fluent Theory Guide-Release 15.0*. ANSYS,Inc, Canonsburg.

Favacho, B.I., 2014. *A mathematical approach applied to the design of naval propeller blades*. Master's thesis, Federal University of Para, BelÃl'm,Brazil.

Gandin, A., 2000. "From constrained to unconstrained growth during directional solidification". *Acta Materialia*, Vol. 48, pp. 2483 – 2501.

Lopes, F.A.C., 2003. "Estimation of mechanical properties and structural analysis via finite element method of naval propellers produced in the amazon".

Loureiro, J.C.S., Oliveira, M.F.S., Pinto, R.O., Rocha, O.F.L., Peralta, J.L. and Moreira, A.L.S., 2000. "Influence of the manufacturing process on the performance of propeller-type marine propellers used by vessels in the amazonian conditions". In *Proceedings of the Brazilian Congress Of Engineering And Materials Science - 14° CBECIMAT*. SÃčo Pedro, Brazil.

Pariona, M.M. and Mossi, A.C., 2005. "Numerical simulation of heat transfer during the solidification of pure iron in sand and mullite molds". *Journal of the Brazilian Society of Mechanical Sciences*, Vol. 27, p. 4.

7. RESPONSIBILITY NOTICE

The authors are the only responsible for the printed material included in this paper.